Int J Adv Manuf Technol (2016) 87:3349–3358
DOI 10.1007/s00170-016-8743-9

ORIGINAL ARTICLE

A parametric study on laser cladding of Ti-6Al-4V wire and WC/W_2C powder

P. K. Farayibi[1] · **T. E. Abioye**[1] · **A. T. Clare**[2]

Received: 26 August 2015 / Accepted: 4 April 2016 / Published online: 14 April 2016

Abstract In this paper, laser cladding of Ti-6Al-4V wire and WC/W_2C powder to produce metal matrix composite clads with a high ceramic reinforcement and a wider clad width was investigated. Taguchi design of experiments and multiple regression models were used to support this. Single clad deposition of Ti-6Al-4V wire and WC/W_2C powder was made on a Ti-6Al-4V substrate using wire and powder co-feeding systems. Clad samples were made at varying processing parameters using L_9 orthogonal experimental matrix data. The clad geometries (height and width) and the weight, obtained using a Talysurf CLI 1000 surface profiler and a weighing scale with a sensitivity of 0.0001 g, were presented and analysed. The results showed that a process condition of 1800 W laser power, 300 mm/min traverse speed, 700 mm/min wire feed rate and 30 g/min powder feed rate produced the composite clads with the highest reinforcement fraction of 76 ± 1 wt%, clad height of 1.57 ± 0.03 mm and clad width of 3.91 ± 0.05 mm. This process condition resulted in a clad with the highest signal to noise ratio of 37.67 for the WC/W_2C reinforcement and the geometrical aspect ratio (H/W) of 0.40 which lies within the range of $0.42 \geq (H/W) \geq 0.13$ to prevent the formation of inter-run porosity in deposited overlap clads. The multiple regression model obtained was able to predict the values of the output characteristics with an accuracy of 92 %. The method employed in this study could be easily implemented when other different materials are investigated to result in the optimisation of the process with fewer experimental runs.

Keywords Laser cladding · Ti-6Al-4V · WC/W_2C · Composite · Taguchi design

✉ A. T. Clare
adam.clare@nottingham.ac.uk

P. K. Farayibi
peterkinjoe105@gmail.com

T. E. Abioye
tennyjoy2003@yahoo.com

[1] Mechanical Engineering Department, Federal University of Technology, Akure PMB 704, Nigeria

[2] Manufacturing Division, Faculty of Engineering, University of Nottingham, University Park, Nottingham NG7 2RD, UK

1 Introduction

Laser cladding is an additive manufacturing technique which involves consolidation of materials with desirable properties fed into a laser-generated melt pool and cools to form a clad layer on a component surface as it solidifies [1, 2]. The controlled repetition of the clad layer formed may result in either the fabrication of a 3-dimensional (3D) component or a surface coating on a component. Laser cladding, as a surface coating technique, allows the use of a premium coating material with superior physical and chemical properties to protect engineering component surfaces in service from wear, corrosion, thermal degradation and impact [3]. Cladding offers advantages such as minimal heat input, precise energy control to a localised region, excellent material utilisation, microstructural control with tailored properties and a well-bonded clad layer over other surface preparations such as tungsten inert gas (TIG), high-velocity oxy-fuel (HVOF), submerged arc (SA) and metal inert gas (MIG) [4, 5].

Metal matrix composites can be easily produced by the introduction of both metal and ceramic feedstocks into the laser-generated melt pool. The development of metal matrix composites (MMCs) are desirable for various engineering applications which may include wear management, thermal

management and enhanced structural stiffness [6]. Moreover, metals such as aluminium and titanium possess good high strength to weight ratio, and excellent ductility and fatigue, but these materials have poor tribological characteristics due to high friction coefficient and low hardness [7]. However, the inclusion of ceramic particles into these metals to form metal matrix composites will enhance their usage for tribological applications. For example, sliding and erosion wear characteristics have been the subject of investigation by [8] and [9], respectively. The result is the enhanced performance of the composite clad compared to the substrated Ti alloy.

In the past, pre-blended powders of Ti and its alloys with WC [10], TiC [8] and SiC [11] particles have been laser deposited for improved wear and hardness properties; however, the powder-based methods, when compared to wire laser cladding, is not as economical in terms of material utilisation, cost of preparation and recovery of unused powder. Hence, wire-based laser cladding may be considered as a more cost-effective process when compared to powder-based process, as material utilisation approaches 100 % with a cleaner process environment [12]. Laser clads of MMCs such as WC/W_2C/Inconel 625 [13] and Ti-6Al-4V/(WC/W_2C) [14] have been successfully deposited by concurrent feeding of wire and powder materials into the laser-generated melt pool. However, this study examined the process conditions required to achieve a metal matrix composite clad with the highest weight percent of the ceramic reinforcement and a wider clad width which is necessary to achieve a surface coating by overlapping clads with no inter-run porosity, as shown in Fig. 1.

In order for inter-run porosity to be eliminated in clad overlaps, it is expected that the clad angle, $\theta°$, should lie between 100° and 150°, and according to Eq. (1) [15], thus substituting the clad angle lower and upper limit values of 100° and 150° into Eq. (1) resulted in (H/W) values of 0.42 and 0.13, respectively. Therefore, clad geometrical aspect ratio (H/W) should be within the range of $0.42 \geq (H/W) \geq 0.13$.

$$\theta^o = 180 - 2\tan^{-1}\left(\frac{2H}{W}\right) \quad (1)$$

In this study, an investigation was carried out by employing Taguchi design of experiment techniques and a regression model to establish the process conditions necessary to prepare surface coatings of metal matrix composite laser clads using Ti-6Al-4V wire and WC/W_2C powder. Furthermore, this method may be used as a basis for devising strategies for any multimaterial laser deposition technique.

2 Experimental

The materials used in this study were a 1.2-mm diameter Ti-6Al-4V wire supplied by VBC Group (Loughborough, UK) and a tungsten carbide powder with a size range of 40–270 μm supplied by Technogenia, France. The powder mean size was measured as 136 μm using laser diffractometry, and its phase constituents were determined as WC and W_2C using X-ray diffraction (XRD) machine. The mean density of the WC/W_2C powder was measured as 16.257 ± 0.007 g/cm^3 using AccuPyc 1330 gas pyncometer. A 0.6:0.4 volume ratio of WC to W_2C was estimated using linear rule of mixture (RoM) with the density of WC taken as 15.7 g/cm^3 and W_2C as 17.1 g/cm^3 [16]. Rectangular, Ti-6Al-4V coupons with dimensions (180 mm × 100 mm × 5 mm) were used as substrates during the cladding process. The coupons were grit blasted with alumina grit to improve laser absorptivity and degreased with acetone to remove contaminants prior to deposition.

A 2-kW ytterbium-doped, continuous wave fibre laser (IPG Photonics) operating at 1.07 μm wavelength was employed for the cladding experiments. The fibre laser was coupled with a beam delivery system (125-mm collimating lens and a 200-mm focusing lens) and a Precitec YC 50 cladding head. The laser configuration was mounted on a CNC table having 4 degrees of freedom to traverse the substrate. A front feeding nozzle coupled with a Redman wire feeder mechanism (Redman Controls and Electronics Ltd., England) was used to deliver the Ti-6Al-4V wire into the melt pool, and the WC/W_2C powder was delivered through a rear feeding nozzle coupled with a model 1264 powder feeder (Praxair Surface Technologies).

The cladding configuration used in this study is schematically shown in Fig. 2. The fibre laser delivers a beam with a Gaussian profile which was defocussed to give a 7.5-mm^2 circular spot area to accommodate materials delivered into

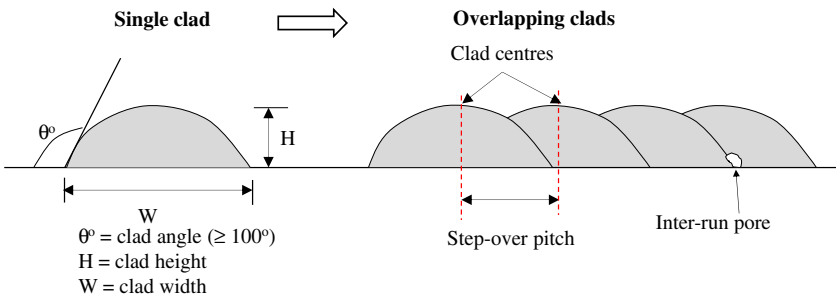

Fig. 1 A schematic of single clad and overlapping clads with geometrical characteristics

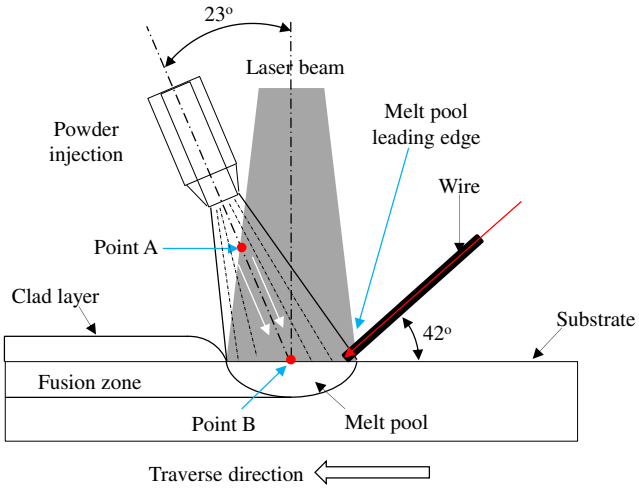

Fig. 2 A schematic of the laser cladding experimental setup

the laser-generated melt pool developed on the Ti-6Al-4V substrate. The working envelope was isolated from the environment using a flexible chamber which was continuously flushed with argon, Ar, at a flow rate of 30 l/min prior to the start of the cladding process and during the experiment to prevent oxidation of deposits. Ar was also supplied to the powder feeder at a flow rate of 10 l/min to serve as a carrier gas for powder delivery into the melt pool. Table 1 contains the list of the selected four process parameters/factors with each parameter having three levels. However, these levels of parameters were selected based on preliminary experiments as the deposition process was stable within these ranges. The ranges of parameters employed during the preliminary experiments were also listed in Table 1.

Owing to a previous observation that there is a partial or no interaction among the process parameters in laser cladding [17, 18], Taguchi experimental design has been chosen to study the direct influence of the process parameters on the desired geometrical characteristics of clad angle, width and height. Taguchi design allows possible combinations of the process parameters with a small number of experimental runs which are statistically appropriate to be conducted to yield the desired results from the process rather than running a full factorial experiment. An L_9 (3^4) orthogonal array was selected to generate the experimental matrix which gives the combination of the process parameters and the number of the experimental runs required. Based on the L_9 (3^4) orthogonal array, nine experimental runs were carried out with three repetitions for each of the experimental treatment/run as shown in Table 2. Columns 2, 3, 4 and 5 were assigned to (A) laser power, W; (B) traverse speed, mm/min; (C) wire feed rate, mm/min; and (D) powder feed rate, g/min, respectively.

The considered outputs under investigation were the clad height, the clad width and the weight percent of the WC/W_2C reinforcement in the deposits. The clad height and width were measured using a Talysurf CLI 1000 profilometer (Taylor Hobson Precision Ltd., UK) in a laser operational mode. The mean height and width of each track were obtained from measurements taken at three different positions in the middle region of each track where deposition was noticed to be steady and stable. The weight percent of the reinforcement in the deposit was obtained by determining the weight difference between the deposited track weight and weight of the Ti-6Al-4V wire deposited.

3 Results and discussion

The preliminary experiments using the ranges of parameters listed in Table 1 led to a choice of three levels for each process parameter employed to establish relationships between clad characteristics (clad height, width and weight fraction of reinforcement) and the selected process factors. The preliminary experiments were conducted according to a combination of

Table 1 Process parameters selected for investigation during the cladding experiments

Process parameters		Levels		
		1	2	3
A	Laser power, LP, W	1400	1600	1800
B	Traverse speed, TS, mm/min	200	300	400
C	Wire feed rate, WFR, mm/min	700	750	800
D	Powder feed rate, PFR, g/min	10	20	30
Ranges of parameters for preliminary experiment				
Laser power (W)	1200–1800			
Traverse speed (mm/min)	100–400			
Wire feed rate (mm/min)	500–800			
Powder feed rate (g/min)	10–40			

Table 2 Experimental matrix for the L_9 (3^4) orthogonal array with four factors and three levels

	Process parameters				Objective functions			Mean (*H*/*W*)
No.	A	B	C	D	S/N_H	S/N_W	$S/N_{WC/W2C}$	
1	1400	200	700	10	−5.28	11.30	35.06	0.50
2	1400	300	750	20	−4.14	10.54	36.14	0.48
3	1400	400	800	30	−3.77	9.34	36.74	0.52
4	1600	200	750	30	−7.24	12.18	37.43	0.57
5	1600	300	800	10	−2.86	11.76	34.55	0.36
6	1600	400	700	20	−1.54	11.17	36.51	0.33
7	1800	200	800	20	−6.66	12.74	36.88	0.49
8	1800	300	700	30	−3.90	11.85	37.67	0.40
9	1800	400	750	10	0.32	12.67	34.78	0.22

parameters generated using an L_{16} orthogonal array, and pictures of some of the deposited tracks are shown in Fig. 3.

Based on tracks 1, 2 and 4 in Fig. 3, a laser power of 1400 W and above was considered suitable to achieve a consistent and stable deposition of the multimaterial system. However, traverse speed less than 200 mm/min and powder feed rate greater than 30 g/min were considered not suitable to achieve a consistent deposition as revealed by track 3. The wire feed rate below 700 mm/min was not considered as suitable as well as revealed by track 5 and others which could not be presented here. This limited the ranges of process parameters to laser power (1400–1800 W), traverse speed (200–400 mm/min), wire feed rate (700–800 mm/min) and powder feed rate (10–30 g/min).

Moreover, during the trial deposition experiments, a deposition strategy was also discovered which promotes stability of the deposition process. The strategy was to start with the deposition of the Ti-6Al-4V wire for some few seconds before the introduction of the WC/W_2C powder into the laser-generated melt pool. Figure 4 shows two tracks which were deposited with the same process conditions employed to demonstrate the effect of the deposition strategy.

Parameters: P = 1800 W, TS = 300 mm/min, WFR = 700 mm/min, PFR = 30 g/min

Fig. 4 Single tracks deposited with the same process conditions **a** deposited with both powder and wire fed at the same time and **b** deposited with wire firstly fed followed by powder injection

Figure 4a showed clad tracks with bumps on the surface while Fig. 4b showed a clad with consistent surface which indicated the stability of the deposition process when wire was deposited for some few seconds before the injection of the reinforcement powder. This consistency was to be attributed to the preheating that may have taken place at the start of the deposition process with the wire fed. Additionally, the laser energy has not been attenuated by the powder stream flowing into the melt pool at the beginning when the wire deposition first started. Thus, with a more voluminous molten pool at high temperature, there should be continuation with the consistency of deposition even with the injection of the powder delivered at a rate within the range specified.

Having identified the ranges of process parameters that support consistent deposition and the L_9 orthogonal array experiment conducted, some of the deposited clad tracks obtained are showed in Fig. 5 and analysis of the characteristics of these clads are further explored.

In Taguchi design, the response of the observations is usually denoted by signal to noise (*S*/*N*) ratio which is expressed in Eq. (2).

$$S/N = -10\log_{10}(\mathrm{MSD}) \tag{2}$$

where S/N = signal to noise ratio and MSD = mean squared deviation

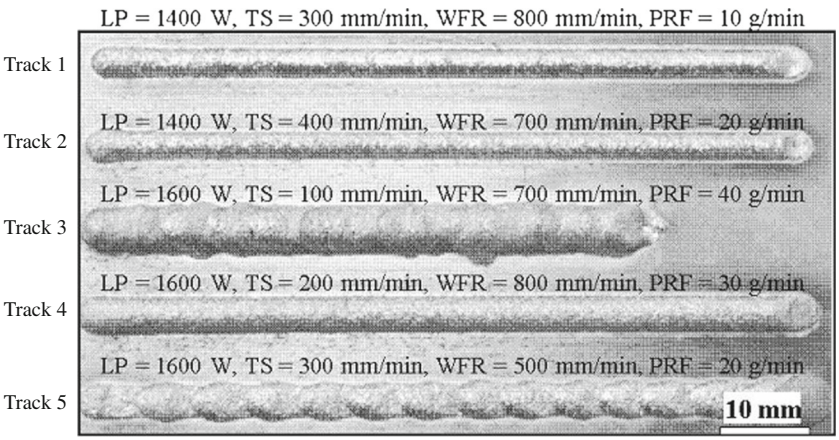

Fig. 3 Single track deposits showing the evolution of stable processing conditions

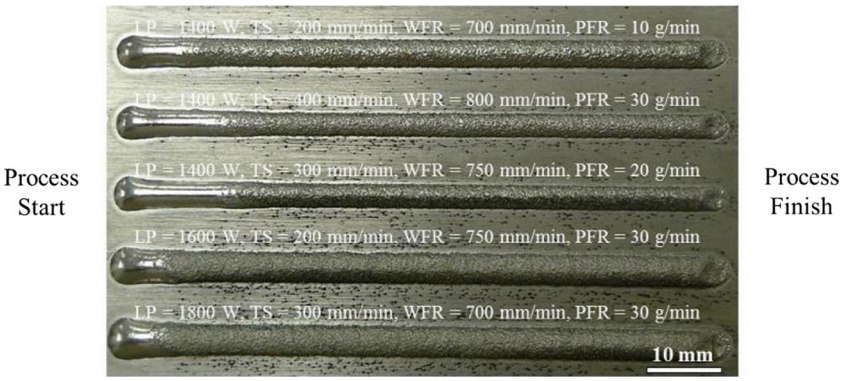

Fig. 5 Selected clads of Ti-6Al-4V/WC/W_2C composites showing a consistent deposition

The mean squared deviation (MSD) is defined differently depending on the chosen geometrical characteristics. Since the deposited tracks of the metal matrix composites were meant to be prepared as hardfacing clads on substrate, a lower clad height is desirable and this output performance is characterised as "the smaller the better" characteristic. However, it is desirable to have a wider clad width, so as to eliminate inter-run porosity when the deposited tracks are overlapped. Also, it is highly desirable to have a higher reinforcement fraction in the metal matrix which is one of the factors necessary for enhanced wear resistance [9, 19]. Thus, "the bigger the better" characteristic is used to characterise both the clad width and the weight percent of the WC/W_2C reinforcement in the composites. The MSDs for the two different types of characteristics are presented in Eqs. (3) and (4).

For the smaller the better,

$$\mathrm{MSD} = \frac{1}{n}\sum_{i=1}^{n} y_i^2 \tag{3}$$

For the bigger the better,

$$\mathrm{MSD} = \frac{1}{n}\sum_{i=1}^{n} \left(\frac{1}{y_i^2}\right) \tag{4}$$

where y_i = result/observation of the experiment at ith trial and n = number of repetitions. Thus, the most significant process parameters influencing the selected response characteristics (clad height, clad width and weight percent of the reinforcement) with their optimum levels can be determined from the *S*/*N* analyses.

In order to determine the main effect of each of the parameters on the output characteristics, the mean value of the outputs obtained from each level of the individual process parameters, presented in columns 6, 7 and 8 in Table 2, were computed and values presented in Table 3. Figure 6 shows the main effect plot of the mean *S*/*N* ratio for the clad height which was obtained using values from Table 3 to indicate the impact of each process parameter level. The increase in two of the process parameters (laser power and traverse speed) supports the decrease in clad height while the increase in wire feed rate and powder feed rate promotes the increase in clad height. However, the clad height is more sensitive to change in traverse speed considering the slope of the linear dependence of the clad height on the each process parameter, as a small increase in the traverse speed significantly decreases the clad height (Fig. 6).

Figure 7 shows the plot of the mean *S*/*N* ratio for the clad width. The increase in only laser power promotes the increase in clad width while the increase in the other three process parameters supports the decrease in the clad width. Moreover, of all the process parameters, a slight increase in laser power significantly increases the width of the deposited clads. This is obvious as the widening of the melt pool is promoted by higher heat intensity.

Table 3 Mean objective function values

Process parameter	S/N_H			S/N_W			$S/N_{WC/W2C}$		
	Levels			Levels			Levels		
	1	2	3	1	2	3	1	2	3
A	−4.40	−3.88	−3.41	10.39	11.7	12.42	35.98	36.16	36.44
B	−6.39	−3.63	−1.66	12.07	11.38	11.06	36.46	36.12	36.01
C	−3.57	−3.69	−4.43	11.44	11.80	11.28	36.41	36.12	36.06
D	−2.61	−4.11	−4.97	11.91	11.48	11.12	34.8	36.51	37.28

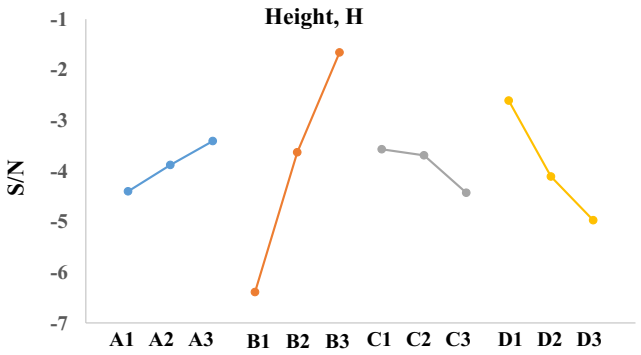

Fig. 6 Main effect plot of mean *S/N* ratio for clad height. The colored dots are significant as they indicate the mean values of *S/N* ratio at different levels of each parameter

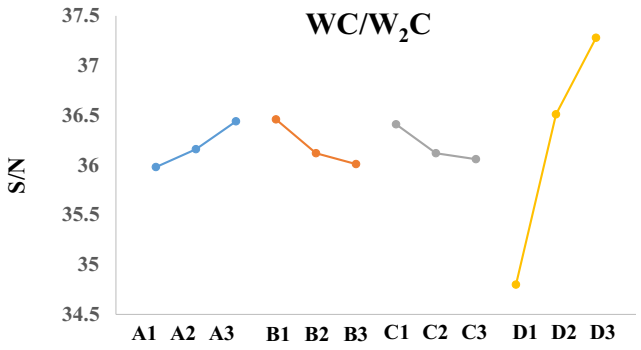

Fig. 8 Main effect plot of mean *S/N* ratio for weight percent of reinforcement. The colored dots are significant as they indicate the mean values of *S/N* ratio at different levels of each parameter

Figure 8 shows the plot of the mean *S/N* ratio for the weight percent of reinforcement in the deposited clad. The increase in two process parameters (laser power and powder feed rate) promotes the increase in the reinforcement fraction of the metal matrix composite formed upon deposition. The increasing weight percent of the ceramic reinforcement is more sensitive to a slight increase in the rate at which WC/W_2C powder is delivered to the laser-generated melt pool. Moreover, process traverse speed and wire feed rate inhibit the increase in the ceramic reinforcement fraction, as their increase results in the decrease in the assimilation of the powder particles into the melt pool during processing.

It is evident that when laser power is increased, the mean clad height decreased while the mean clad width and the mean weight percent of reinforcement increased. Increasing traverse speed results in decreasing clad height, clad width and weight percent of reinforcement. While clad width seemed not to be affected by the changes in wire feed rate, increasing wire feed rate results in increasing clad height and decreasing weight percent of reinforcement. It is obvious that increasing powder feed rate results in increasing weight percent of reinforcement in the deposits and clad height; however, clad width decreases.

Analysis of variances (ANOVA) for the output characteristics was performed to determine the relative importance of the process parameters. Table 4 presents the summary of the ANOVA analyses for clad height, width and weight percent of reinforcement.

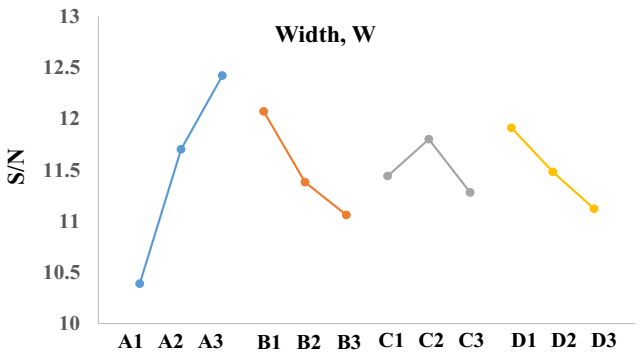

Fig. 7 Main effect plot of mean *S/N* ratio for clad width. The colored dots are significant as they indicate the mean values of *S/N* ratio at different levels of each parameter

The ANOVA analysis shows that the process traverse speed affects clad height by approximately 79 % and laser power affects clad width by approximately 68 % while powder feed rate employed affects the weight percent of reinforcement by about 89 %.

Thus, it can be inferred that in order for a deposited composite clad to possess a geometrical aspect ratio (H/W) within a range of $0.42 \geq (H/W) \geq 0.13$ and high weight fraction of reinforcement, a high laser power (1800 W) and a high powder flow rate (30 g/min) are required. In Table 2, the 8th treatment delivered the highest signal to noise ratio of 37.67 for the WC/W_2C reinforcement and also the geometrical aspect ratio of the clad formed (0.40) falls within the required range. Hence, a process condition of 1800 W laser power, 300 mm/min traverse speed, 700 mm/min wire feed rate and 30 g/min powder feed rate is required to deposit the best composite clads with the reinforcement fraction of 76 ± 1 wt%, clad height of 1.57 ± 0.03 mm and clad width of 3.91 ± 0.05 mm. This best composite clad was achieved as a result of the maximum laser power (1800 W) employed which resulted in the highest signal to noise ratio for clad width as shown in Fig. 7. This indicated that using 1800 W laser power, a wider melt pool is achieved which facilitated increased assimilation of the ceramic reinforcement particles exposed to the melt pool surface. Thus, the laser power of 1800 W encouraged the wider composite clads with a high reinforcement fraction to be achieved. Moreover, employing a powder flow rate of 30 g/min resulted in achieving a maximum signal to noise ratio for percentage reinforcement in deposited clads as shown in Fig. 8. Thus, this further supports the reason for the best composite clad with as high as 76 ± 1 wt% ceramic reinforcement to be achieved, coupled with a wider melt pool size generated by the maximum laser power of 1800 W. Figure 9 shows the cross sections of the deposited clads with insert

Table 4 Analysis of variance for clad height, width, and weight percent of WC/W_2C reinforcement

Process parameter	DOF	Clad height			Clad width			Weight percent of WC/W_2C		
		SS	MS	%	SS	MS	%	SS	MS	%
A	2	0.05	0.02	1.07	3.34	1.672	67.91	68.60	34.30	3.79
B	2	3.49	1.75	78.66	0.79	0.394	15.77	56.55	28.27	3.10
C	2	0.12	0.06	2.70	0.21	0.104	3.94	36.01	18.00	1.91
D	2	0.76	0.38	17.10	0.42	0.211	8.29	1543.15	771.57	88.99
Error	18	0.01	0.001	0.47	0.14	0.008	4.09	26.44	1469.00	2.21
Total	26	4.43		100	4.90		100	1730.75		100

labelled "(h)" as the best composite clad, and Fig. 10 shows a cross-sectional view of the overlapping clads deposited, with the parameters which gave the best reinforcement fraction and H/W of 0.4 (Fig. 9), without inter-run porosity.

3.1 Regression modelling and evaluation

In order to be able to make a numerical prediction of the output characteristics within the range of each process parameters based on the experimental responses obtained for the clad height, the clad width and the weight percent of reinforcement, multiple linear regression model was employed which can be generally expressed as shown in Eq. (5).

$$y = \beta_0 + \beta_1 A + \beta_2 B + \beta_3 C + \beta_4 D \tag{5}$$

where y is the output characteristic, (β_0, β_1, β_2, β_3, β_4) are the regression coefficients and (A, B, C, D) are the process parameters.

In multiple linear regression modelling, since there are five (5) regression coefficients to be determined, five sets of equations need to be developed and simultaneously solved to

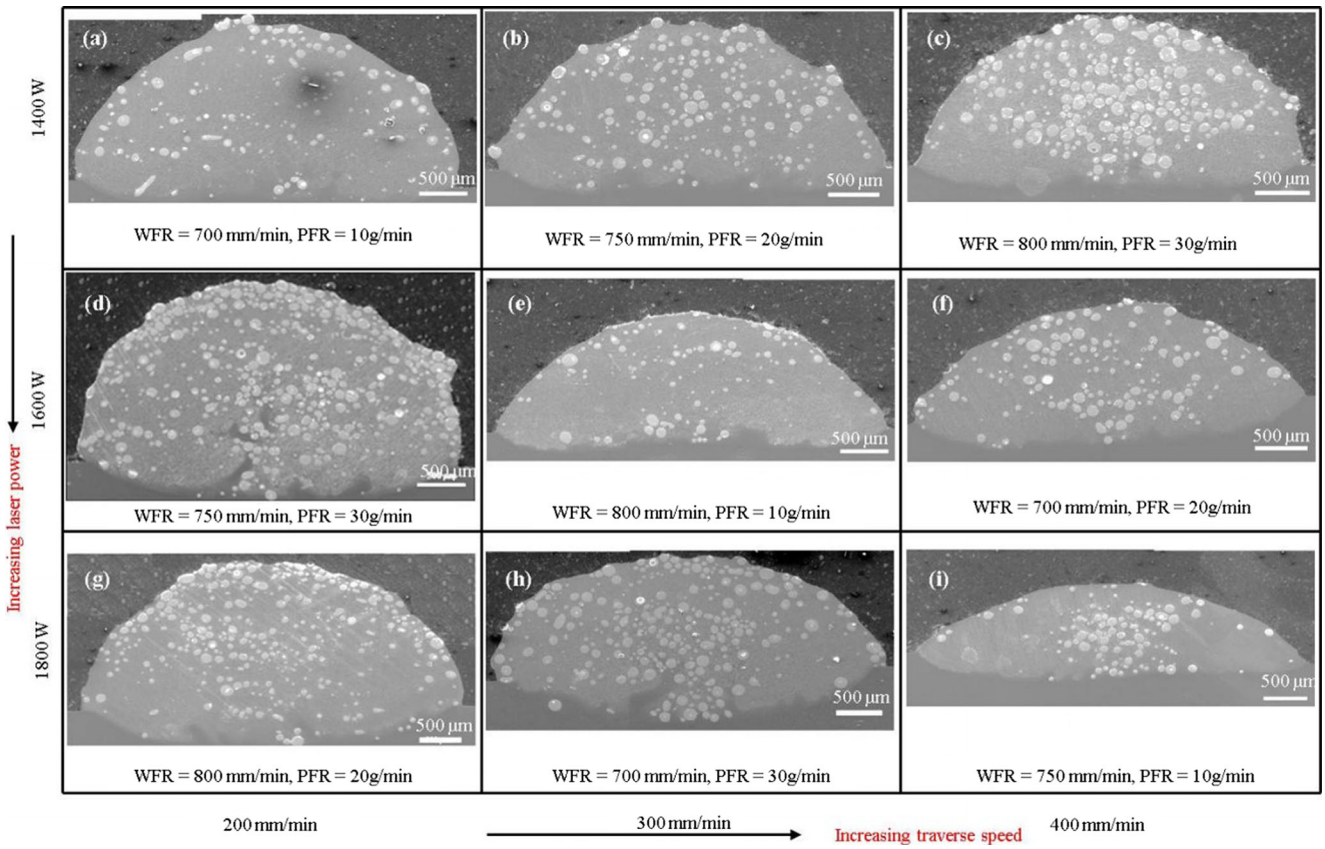

Fig. 9 BSE-SEM of Ti-6Al-4V/WC/W2C composite clad cross sections (white features are WC/W2C particles in cross section)

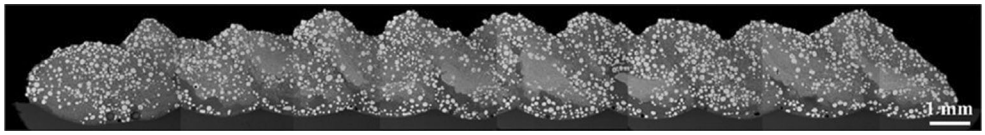

Fig. 10 A cross-sectional view of overlap clads containing the highest reinforcement weight percent

obtain the values of the coefficient. Considering the treatments presented in Table 2 and observed values of the responses in Table 6, the set of equations can be obtained from the following expressions:

$$
\begin{aligned}
&n\ \beta_0 + \beta_1\sum_{i=1}^{n} A + \beta_2\sum_{i=1}^{n} B + \beta_3\sum_{i=1}^{n} C + \beta_4\sum_{i=1}^{n} D = \sum_{i=1}^{n} y\\
&\beta_0\sum_{i=1}^{n} A + \beta_1\sum_{i=1}^{n} \left(A^2\right) + \beta_2\sum_{i=1}^{n} (AB) + \beta_3\sum_{i=1}^{n} (AC) + \beta_4\sum_{i=1}^{n} (AD) = \sum_{i=1}^{n} (Ay)\\
&\beta_0\sum_{i=1}^{n} (B) + \beta_1\sum_{i=1}^{n} (AB) + \beta_2\sum_{i=1}^{n} \left(B^2\right) + \beta_3\sum_{i=1}^{n} (BC) + \beta_4\sum_{i=1}^{n} (BD) = \sum_{i=1}^{n} (By)\\
&\beta_0\sum_{i=1}^{n} (C) + \beta_1\sum_{i=1}^{n} (AC) + \beta_2\sum_{i=1}^{n} (BC) + \beta_3\sum_{i=1}^{n} \left(C^2\right) + \beta_4\sum_{i=1}^{n} (CD) = \sum_{i=1}^{n} (Cy)\\
&\beta_0\sum_{i=1}^{n} (D) + \beta_1\sum_{i=1}^{n} (AD) + \beta_2\sum_{i=1}^{n} (BD) + \beta_3\sum_{i=1}^{n} (CD) + \beta_4\sum_{i=1}^{n} \left(D^2\right) = \sum_{i=1}^{n} (Dy)
\end{aligned}
$$

where n is the number of treatments. Thus, determining the set of equation for clad height to obtain the regression coefficient for this response characteristic, the following set of equations are obtained:

$$
\begin{aligned}
&9\ \beta_0 + 14400\ \beta_1 + 2700\ \beta_2 + 6750\ \beta_3 + 180\ \beta_4 = 14.55\\
&14400\beta_0 + 23280000\beta_1 + 4320000\beta_2 + 10800000\beta_3 + 288000\beta_4 = 23218\\
&2700\ \beta_0 + 4320000\ \beta_1 + 870000\ \beta_2 + 2025000\ \beta_3 + 54000\ \beta_4 = 4105\\
&6750\beta_0 + 10800000\beta_1 + 2025000\beta_2 + 5077500\beta_3 + 135000\beta_4 = 10936.5\\
&180\ \beta_0 + 288000\ \beta_1 + 54000\ \beta_2 + 135000\ \beta_3 + 4200\ \beta_4 = 303.2
\end{aligned}
$$

Thus, solving the system of equations simultaneously which may be presented in a matrix form $\alpha\beta=\gamma$, where α is a (5×5) matrix representing the coefficients of βs in the set of equations, β is a (5×1) matrix representing the regression coefficients to be determined and γ is a (5×1) matrix representing the solutions to the set of equations. Thus, the solution to this set of equations is

$$\beta_0 = 1.7; \beta_1 = -0.000256; \beta_2 = -0.00433; \beta_3 = 0.00164;\ \text{and}\ \beta_4 = 0.0203$$

Therefore, the fitted multiple regression equation for clad height is

$$\text{Clad Height, } H\ (\text{mm}) = 1.7 - 0.000256\text{A} - 0.00433\text{B} + 0.00164\text{C} + 0.0203\text{D}$$

Moreover, regression equations relating the process parameters and the other output characteristics (clad width and weight percent of reinforcement) are obtained and the regression coefficients for each observed response are presented in Table 5.

Table 5 Coefficients of the regression equation for the output characteristics

Regression coefficients	β_0	β_1 ($\times10^{-4}$)	β_2 ($\times10^{-3}$)	β_3 ($\times10^{-4}$)	β_4 ($\times10^{-2}$)
Clad height (mm)	1.70	−2.56	−4.33	16.40	2.03
Clad width (mm)	1.41	21.40	−2.00	−1.74	−1.53
WC/W_2C (wt%)	56.2	97.50	−17.40	−263.00	91.10

Table 6 Percentage differences between the predicted and observed values of the output characteristics

Treatment		1	2	3	4	5	6	7	8	9
Clad height (mm)	Observed value	1.84	1.61	1.54	2.3	1.39	1.19	2.15	1.57	0.96
	Predicted value	1.82	1.67	1.52	2.25	1.49	1.10	2.08	1.68	0.93
	Difference (%)	1.09	3.72	1.30	2.17	7.19	7.56	3.26	7.01	3.13
Clad width (mm)	Observed value	3.67	3.37	2.95	4.06	3.87	3.62	4.34	3.91	4.30
	Predicted value	3.73	3.37	3.00	3.84	3.94	3.61	4.42	4.08	4.18
	Difference (%)	1.63	0.00	1.69	5.42	1.81	0.28	1.84	4.35	2.79
WC/W_2C (wt%)	Observed value	56.63	64.1	68.73	74.43	53.50	66.9	69.87	76.47	54.83
	Predicted value	57.07	63.13	69.18	75.92	54.65	64.65	67.45	77.45	56.17
	Difference (%)	0.78	1.51	0.65	2.00	2.15	3.36	3.46	1.28	2.44

The values of the regression coefficients of the process parameters further support the main effect of each of the process parameters on the output characteristics. Moreover, for other multimaterial systems, similar relationships are expected within their specified deposition parameter ranges.

Table 6 shows the percentage differences between the predicted values for the output characteristics obtained from the multiple regression equations and their observed values. It was observed that the deviation from the observed values for all the output characteristics is less than 8 % which indicates that the multiple regression models can predict to an accuracy of 92 %. However, this accuracy can be improved by employing more efficient material delivery systems which would deliver consistently the pre-set material volumes into the melt pool and also by proper alignment of the material delivery nozzles with the melt pool.

4 Conclusions

The composite laser cladding of Ti-6Al-4V wire and WC/W_2C powder has been successfully investigated for the production of surface coating on Ti-based alloys using the Taguchi technique and a regression model. For the material system investigated, a process condition of 1800 W laser power, 300 mm/min traverse speed, 700 mm/min wire feed rate and 30 g/min powder feed rate is required to deposit composite clads with the highest reinforcement fraction of 76 ± 1 wt%, clad height of 1.57 ± 0.03 mm and clad width of 3.91 ± 0.05 mm. This process condition delivered a clad with the highest signal to noise ratio of 37.67 for the WC/W_2C reinforcement and the geometrical aspect ratio (H/W) of 0.40 which lies within the range of $0.42 \geq (H/W) \geq 0.13$ to prevent the formation of inter-run porosity in deposited overlap clads. The experimental design indicated that increasing the laser power most significantly increases the clad width, decreasing traverse speed increases the deposit clad height and powder feed rate obviously influenced the weight percent of reinforcement in the deposits by about 89 %. The multiple regression model was found to be able to predict as accurate as 92 %, which can be improved by efficient material delivery and proper alignment with the melt pool. This method can be easily implemented for the optimisation of any other multimaterial laser deposition.

References

1. Steen W (2003) Laser material processing. Springer-Verlag, London
2. Ion J (2005) Laser processing of engineering materials, principle, procedure and industrial application. Elsevier Butterworth Heinemann, Oxford, London
3. Huang F, Jiang Z, Liu X, Lian J, Chen L (2009) Microstructure and properties of thin wall by laser cladding forming. J Mater Process Technol 209(11):4970–4976
4. Palcic I, Balazic M, Milfelner M, Buchmeister B (2009) Potential of laser engineered net shaping (LENS) technology. Mater Manuf Process 24(7-8):750–753
5. Mok S, Bi G, Folkes J, Pashby I (2008) Deposition of Ti-6Al-4V using a high power diode laser and wire, part I: investigation on the process characteristics. Surf Coat Technol 202(16): 3933–3939
6. Miracle DB, Donaldson SL (2001) Aeronautical applications of metal matrix composites. ASM International, Materials Park, Ohio
7. Huang C, Zhang Y, Vilar R (2011) Microstructure characterisation of laser clad TiVCrASi high entropy alloy coating on Ti-6Al-4V substrate. Adv Mater Res 154–155:621–625
8. Vreeling J, Ocelik V, De Hosson J (2002) Ti-6Al-4V strengthened by laser melt injection of WCp particles. Acta Mater 50(19):4913–4924
9. Farayibi PK, Murray J, Huang L, Boud F, Kinnell P, Clare A (2014) Erosion resistance of laser clad Ti-6Al-4V/WC composite for waterjet tooling. J Mater Process Technol 214(3): 710–721
10. Farayibi PK, Folkes J, Clare A, Oyelola O (2011) Cladding of pre-blended Ti-6Al-4V and WC powder for wear resistant applications. Surf Coat Technol 206(2-3):372–377
11. Chen Y, Liu D, Li F, Li L (2008) WCp/Ti-6Al-4V graded metal matrix composite layer produced by laser melt injection. Surf Coat Technol 202(19):4780–4787

12. Abioye TE, Folkes J, Clare A (2013) A parametric study of Inconel 625 wire laser deposition. J Mater Process Technol 213(12):2145–2151
13. Abioye TE, Folkes J, Clare A, McCartney D (2013) Concurrent Inconel 625 and WC powder laser cladding: process stability and microstructural characterisation. Surf Eng 29(9):647–653
14. Farayibi PK, Folkes J, Clare A (2013) Laser deposition of Ti–6Al–4V wire with WC powder for functionally graded components. Mater Manuf Process 28:514–518
15. De Oliveira U, Ocelik V, De Hosson J (2005) Analysis of coaxial laser cladding processing conditions. Surf Coat Technol 197(2-3): 127–136
16. Ross B (1992) Metallic materials specification handbook, 4th edn. Boundary Row, Chapman and Hall, London, pp 2–6
17. Mazumder J (1996) Laser assisted surface coatings in metallurgical and ceramic protective coatings. In: Stern K (ed) Chapman and Hall, London, p 341
18. Tellez A (2010) Fibre laser metal deposition with wire: parameter study and temperature control. PhD thesis, University of Nottingham, UK
19. Ocelik V, Matthews D, De Hosson J (2005) Sliding wear resistance of metal matrix composite layers prepared by high power laser. Surf Coat Technol 197(23):303–315